Amplitude and time course of evoked and spontaneous synaptic currents in rat submandibular ganglion cells

Robert J. Callister and Bruce Walmsley*

The Neuroscience Group, Discipline of Medical Biochemistry, Faculty of Medicine, The University of Newcastle, Callaghan, NSW 2308, Australia

1. Excitatory postsynaptic currents (EPSCs) were recorded in rat submandibular ganglion cells *in vitro* using the two-electrode voltage clamp technique.

2. The peak amplitude of EPSCs evoked by nerve impulses in single presynaptic fibres varied between 1·2 and 9·8 nA in different cells (mean = 4·6 ± 2·6 nA; $n = 23$; −80 mV membrane potential; 22–25 °C).

3. Experiments were performed to re-investigate a previous hypothesis that different mechanisms underlie the generation of evoked *versus* spontaneous quantal EPSCs in submandibular cells. This hypothesis was based on the observation of different time courses of evoked and spontaneous EPSCs.

4. In agreement with previous studies, the time course of the decay phase of evoked EPSCs was described by the sum of two exponentials, with time constants τ_1 and τ_2 of 6·9 ± 0·7 and 34·4 ± 7·7 ms, respectively ($n = 23$; −80 mV membrane potential).

5. The double-exponential decay of evoked EPSCs persisted when transmitter release was reduced by bath addition of 100 μM cadmium chloride to the level of failures, one or several quanta.

6. Spontaneous EPSCs exhibited mean amplitudes of 81 ± 24 pA ($n = 5$ cells; −80 mV membrane potential), and displayed an extremely wide range of peak amplitudes in the same cell (mean coefficient of variation (c.v.) = 0·37 ± 0·09; $n = 5$ cells). In contrast to a previous report (see below), the decay phase of spontaneous EPSCs was found to exhibit a double-exponential time course with time constants similar to those of the evoked EPSC recorded in the same cell.

7. These results indicate that evoked and spontaneously released quanta of transmitter most probably act on the same population of postsynaptic receptors in submandibular ganglion cells. There is a large variability in the peak amplitudes of quantal EPSCs recorded in the same cell. This large variability is not due to electrotonic effects, since these cells lack dendrites.

Electrophysiological investigations into the quantal nature of synaptic transmission are usually complicated by many factors, including the electrotonic attenuation of synaptic currents generated in the dendritic branches of a neurone, stimulation of multiple-fibre synaptic inputs, and the inability to correlate the origin of spontaneous synaptic currents with specific presynaptic inputs.

In the present study we have used the submandibular ganglion preparation to avoid these serious problems and investigate quantal synaptic transmission at a neuronal nicotinic synapse (Ascher, Large & Rang, 1979; Rang, 1981; Yawo, 1989; Sargent, 1993). This ganglion was chosen because, firstly, in adult animals 75% of ganglion cells receive input from a single presynaptic axon (Lichtman, 1977). Secondly, there are no interneurones or other sources of intrinsic synaptic input to these cells (Kawa & Roper, 1984). Therefore, both evoked and spontaneous transmitter release occur at a population of release sites arising from the same presynaptic nerve fibre. Thirdly, submandibular ganglion cells are electronically compact because they lack dendrites (Lichtman, 1977).

In a previous study of submandibular ganglion cells, Rang (1981) reported that the spontaneous excitatory post-synaptic currents (EPSCs) exhibit a time course very different from that of the evoked EPSC. The decay time course of the evoked EPSC could be described by the sum

* To whom correspondence should be addressed.

of two exponentials, exhibiting time constants consistent with the two kinetic components of acetylcholine-induced noise in these cells (Rang, 1981; Yawo, 1989). However, the decay time course of the spontaneous EPSCs exhibited only a single exponential time constant, corresponding to the fast time constant of the evoked response. It was concluded that there were two distinct types of channels in the postsynaptic membrane. It was further proposed that these channels are spatially arranged in the postsynaptic membrane, such that both receptor-channel types are accessible only to nerve-evoked quantal release, and only one population is activated by spontaneously released quanta of transmitter (Rang, 1981). *If correct, this hypothesis seriously challenges the use of spontaneous EPSCs to interpret nerve-evoked transmission at neuronal synapses.*

In the present study we have investigated quantal transmission in submandibular ganglion cells using the two-electrode voltage clamp technique. We have also re-examined the hypothesis that evoked and spontaneous quantal EPSCs are generated by different populations of postsynaptic channels in these cells.

Some of this work has been presented in abstract form (Callister & Walmsley, 1994*a*, *b*; Callister, Keast & Walmsley, 1995).

METHODS

Tissue preparation

All experiments were perfomed on the rat submandibular ganglion preparation, as originally described by Lichtman (1977). The preparation consists of a thin triangular sheet of connective tissue stretching between the lingual nerve and the salivary ducts. Neurones providing parasympathetic innervation to the salivary glands lie in the connective tissue sheet and along the salivary ducts. These neurones are innervated by preganglionic axons which leave the brainstem in the chorda tympani nerve and merge with the lingual nerve. Approximately 5–8 mm of the chorda tympani nerve was removed with each preparation for subsequent stimulation.

Wistar rats (5–7 weeks old) were overdosed with halothane and decapitated. The preparation was removed and pinned out in a small Sylgard-lined recording chamber, perfused with a modified Krebs solution and viewed under an inverted microscope. The perfusing solution consisted of (mM): NaCl, 120; $NaHCO_3$, 25; KCl, 5; $MgCl_2$, 2; NaH_2PO_4, 1; $CaCl_2$, 2·5; glucose, 11. The solution was continually bubbled with 95% O_2–5% CO_2 to maintain a pH of 7·3. In some experiments transmitter release was reduced by adding 100 μM cadmium chloride to this solution. All experiments were carried out at 22–25 °C.

Recording and analysis

Synaptic currents and potentials were recorded with an Axoclamp-2A amplifier (Axon Instruments) using the conventional two-electrode voltage clamp technique. The chorda tympani nerve was drawn into a close fitting suction electrode and activated by suprathreshold pulses (0·2 ms, 5–20 V) delivered at a rate of 1–4 Hz. Cells were judged to receive a single presynaptic input if they exhibited an all-or-nothing EPSC in response to finely graded stimulus strength. Recording and current-passing electrodes had resistances of 50–100 MΩ when filled with 4 M potassium acetate and 0·5 M potassium sulphate, respectively. In some experiments synaptic potentials were recorded with a single microelectrode (30–50 MΩ resistance when filled with 0·5 M KCl).

Visualized neurones in the thin connective sheet between the salivary ducts and lingual nerve were impaled with two microelectrodes. A grounded shield was positioned between the tips of the two microelectrodes to reduce capacitive coupling between the electrodes. The voltage clamp was optimized by monitoring the current response to a repetitive voltage step (10 ms, 20 mV). Voltage and current recordings were filtered at 10 and 1 kHz, respectively, and stored on a PCM video recorder (A. R. Vetter Co., Rebersburg, PA, USA). Current records were subsequently filtered off-line at 0·3–1·0 kHz, digitized and analysed using custom-designed programs and software kindly provided by J. Dempster (Strathclyde Electrophysiology Software, Glasgow, UK). The detection and averaging of spontaneous events was performed using SCAN software (J. Dempster, Strathclyde Electrophysiology Software, Glasgow, UK). The detection of spontaneous events was by amplitude threshold, set in each cell to exclude all obvious noise records. Following detection, spontaneous currents were aligned using the mid-point of their rising phases before averaging. The decay phase of each averaged synaptic current was fitted by the sum of two exponentials over a time period following the peak of approximately 100–150 ms. Due to the small variability in 10–90% rise times (standard error of the mean (S.E.M.), 0·1–0·2 ms) of the spontaneous currents, slight differences in the alignment of spontaneous currents prior to averaging would not have any significant effect on the calculations of the decay time constants, which were approximately 7 and 35 ms.

All results are expressed as means ± standard deviation (S.D.). The coefficient of variation (C.V.) is the S.D. divided by the mean. Data were considered to be statistically significant following regression and Student's t test analysis if $P < 0{\cdot}05$.

RESULTS

Two-electrode voltage clamp recordings were made from forty-one cells in twenty-five preparations. Detailed analysis was performed on cells with stable resting membrane potentials more negative than −45 mV. Membrane potentials were usually clamped at values between −50 and −80 mV, with maximum holding currents not exceeding 1 nA. In voltage clamp mode, only cells in which the residual voltage was less than 10% of the unclamped voltage were accepted for further analysis.

Properties of evoked EPSCs

The general features of single-fibre EPSCs evoked in submandibular ganglion cells are illustrated in Fig. 1. Stimulation of the chorda tympani nerve produced a large-amplitude EPSC (Fig. 1*A*) following a delay from the stimulus of 5–23 ms in different cells (mean = 12·3 ± 5·0 ms; $n = 39$). At a membrane potential of −80 mV, EPSCs exhibited a rapid rising phase (10–90% rise time = 2·6 ± 0·4 ms; $n = 16$), followed by a slower decay phase.

The peak amplitude of the EPSC varied linearly with membrane potential for the range of holding potentials between −40 and −80 mV (Fig. 1*B*). Extrapolation of a linear regression line fitted over this range revealed a reversal potential of −9 ± 5 mV ($n = 4$ cells). This value agrees with that previously reported for submandibular ganglion cells in rodents (Rang, 1981; Yawo, 1989), as well as those reported for different autonomic ganglion cell types (Kuba & Nishi, 1979; Derkach, Selyanko & Skok, 1983; Mathie, Cull-Candy & Colquhoun, 1987), consistent with the postsynaptic activation of non-specific cation channels.

Figure 1*C* shows an evoked EPSC recorded at a membrane potential of −80 mV. The decay phase of the EPSC could not be adequately fitted by a single exponential, but was well described by the sum of two exponentials (Fig. 1*C*, ○). As illustrated in the semilogarithmic plot of this EPSC (Fig. 1*D*), the initial rapid decay phase has a time constant of 7·8 ms (τ_1), while the slow phase has a time constant of 31·0 ms (τ_2). This two-phase decay was present in *all* of the evoked EPSCs examined at membrane potentials between −50 and −80 mV (Table 1). In twenty-three cells at a membrane potential of −80 mV, the values for τ_1 ranged from 5·9 to 8·7 ms (mean = 6·9 ± 0·8 ms), while τ_2 ranged from 23·2 to 55·3 ms (mean = 34·4 ± 7·7 ms).

Variability in the amplitude of evoked EPSCs

The mean peak amplitude of evoked EPSCs recorded in submandibular cells varied over a large range (Table 1). At a membrane potential of −80 mV, EPSC peak amplitudes ranged from 1·22 to 9·78 nA (mean = 4·64 ± 2·63 nA; $n = 23$ cells). In individual cells the amplitude of evoked EPSCs fluctuated markedly from trial to trial (Fig. 2*A*). A plot of EPSC peak amplitudes for 500 consecutive trials is shown in Fig. 2*B*. This plot indicates that the fluctuation pattern is stable over time. A histogram of EPSC peak amplitudes is illustrated in Fig. 2*C*. The peak amplitude of

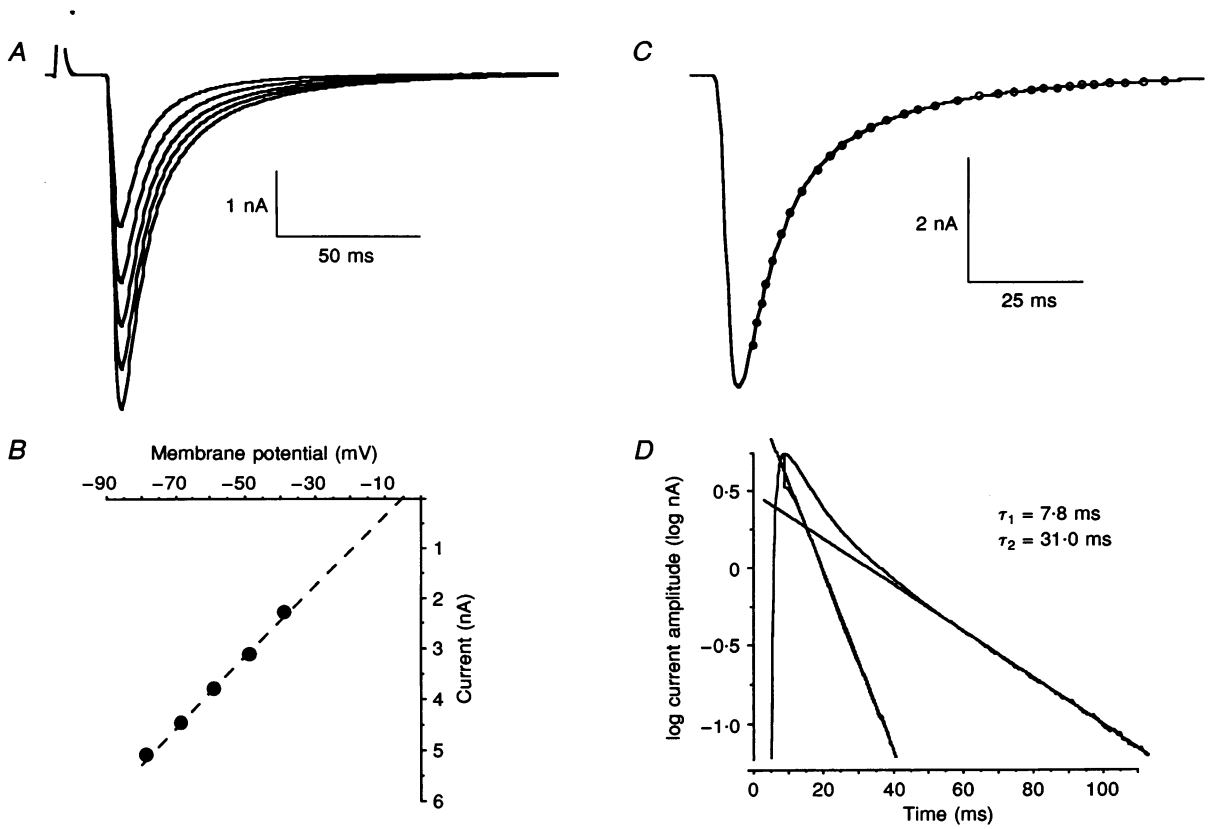

Figure 1. Single-fibre EPSCs evoked in a submandibular ganglion cell

A, EPSCs recorded at a series of increasingly negative membrane potentials: −40, −50, −60, −70 and −80 mV. Each trace represents the average of 100 responses to stimuli delivered at 3·67 Hz. *B*, plot of the peak amplitude of evoked EPSCs *versus* membrane potential. *C*, average evoked EPSC recorded at a membrane potential of −80 mV. The EPSC has a 10–90% rise time of 1·94 ms and the decay phase is well fitted by the sum of two exponentials (○) with time constants of 7·8 and 31·0 ms, respectively. *D*, semilogarithmic plot of the decay phase of the record shown in *C*. The slow exponential component (straight line, upper plot) is superimposed on the average EPSC record. The difference between this slow exponential and the EPSC is also illustrated (lower plot), together with the fast exponential component (straight line).

Table 1. Properties of evoked EPSCs in submandibular ganglion cells

Membrane potential (mV)	EPSC peak amplitude (nA)	Coefficient of variation *	τ_1 (ms)	τ_2 (ms)
−50	2·66 ± 1·30	0·128 ± 0·047 ($n = 5$)	6·9 ± 1·25	30·8 ± 6·0
−60	3·51 ± 1·54	0·145 ± 0·079 ($n = 5$)	6·8 ± 0·8	37·1 ± 12·9
−80	4·64 ± 2·63	0·121 ± 0·044 ($n = 18$)	6·9 ± 0·7	34·4 ± 7·7

Data are from 14, 6 and 23 cells held at membrane potentials of −50, −60 and −80 mV, respectively. All data obtained at room temperature (22–25 °C) in normal Krebs solution (2·5 mM $CaCl_2$). The decay phase of each EPSC was fitted by the sum of two exponentials with time constants τ_1 and τ_2. Values are presented as means ± S.D. * Based on 100–500 responses. The c.v. for EPSC peak amplitude was not obtained for cells where the averaged synaptic current was measured on-line; n denotes number of cells analysed.

the evoked EPSC in this cell fluctuated over a large range with a c.v. of 0·15. The average c.v. for peak EPSC amplitudes was approximately 0·13 for all cells examined ($n = 28$; see Table 1). There is an inverse relationship between the c.v. and the mean peak amplitude of evoked EPSCs. This relationship was statistically significant (regression analysis, $P < 0·05$) for cells held at membrane potentials of −50, −60 and −80 mV and is illustrated for cells held at −80 mV, in Fig. 2*D*. A likely explanation for this inverse correlation is that smaller EPSCs are generated at connections with fewer release sites.

Properties of quantal EPSCs

The only previous study on quantal currents in submandibular ganglion cells reported that the time course of decay of evoked and spontaneous EPSCs is very different

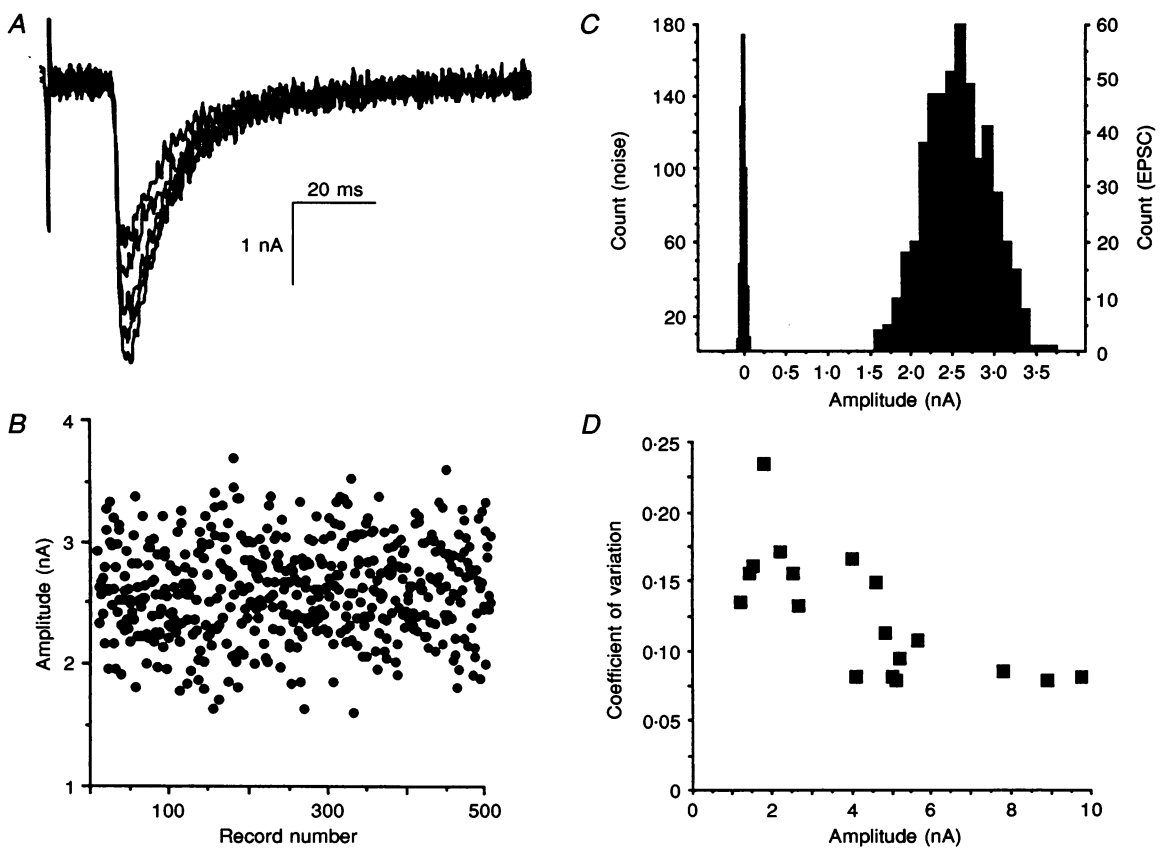

Figure 2. Amplitude fluctuations in evoked EPSCs

A, 5 superimposed EPSCs recorded in a cell following stimulation of the chorda tympani nerve at 2·67 Hz (holding potential, −60 mV). *B*, plot of peak amplitudes of successive EPSCs for 500 trials (same cell as illustrated in *A*). *C*, histogram of EPSC peak amplitudes (right) and corresponding noise (left). *D*, inverse relationship between the coefficient of variation and average peak amplitude of evoked EPSCs demonstrated for 18 cells at a membrane potential of −80 mV.

(Rang, 1981). We have investigated this result further using two strategies. Firstly, we compared the time course of evoked EPSCs with that obtained under conditions in which release had been reduced to the level of failures or few quanta. Secondly, we compared the time course of evoked and spontaneous quantal EPSCs in the same cell.

Evoked quantal EPSCs recorded in the presence of cadmium chloride.

The quantal content of the evoked synaptic response was reduced to the level of failures by adding cadmium chloride to the perfusate to block presynaptic calcium currents. In preliminary experiments we used a single microelectrode (30–80 MΩ) to record evoked EPSPs. A cadmium chloride concentration of 100 μM was found to be optimal for reducing the amplitude of the evoked EPSPs to the level of clear failures and one or several quanta.

Based on these findings we subsequently obtained two-electrode voltage clamp recordings of evoked EPSCs in the presence of 100 μM cadmium chloride. The results of one such experiment are shown in Fig. 3. Over the course of several minutes the evoked EPSC (Fig. 3*A*) progressively decreased to a level at which failures of response

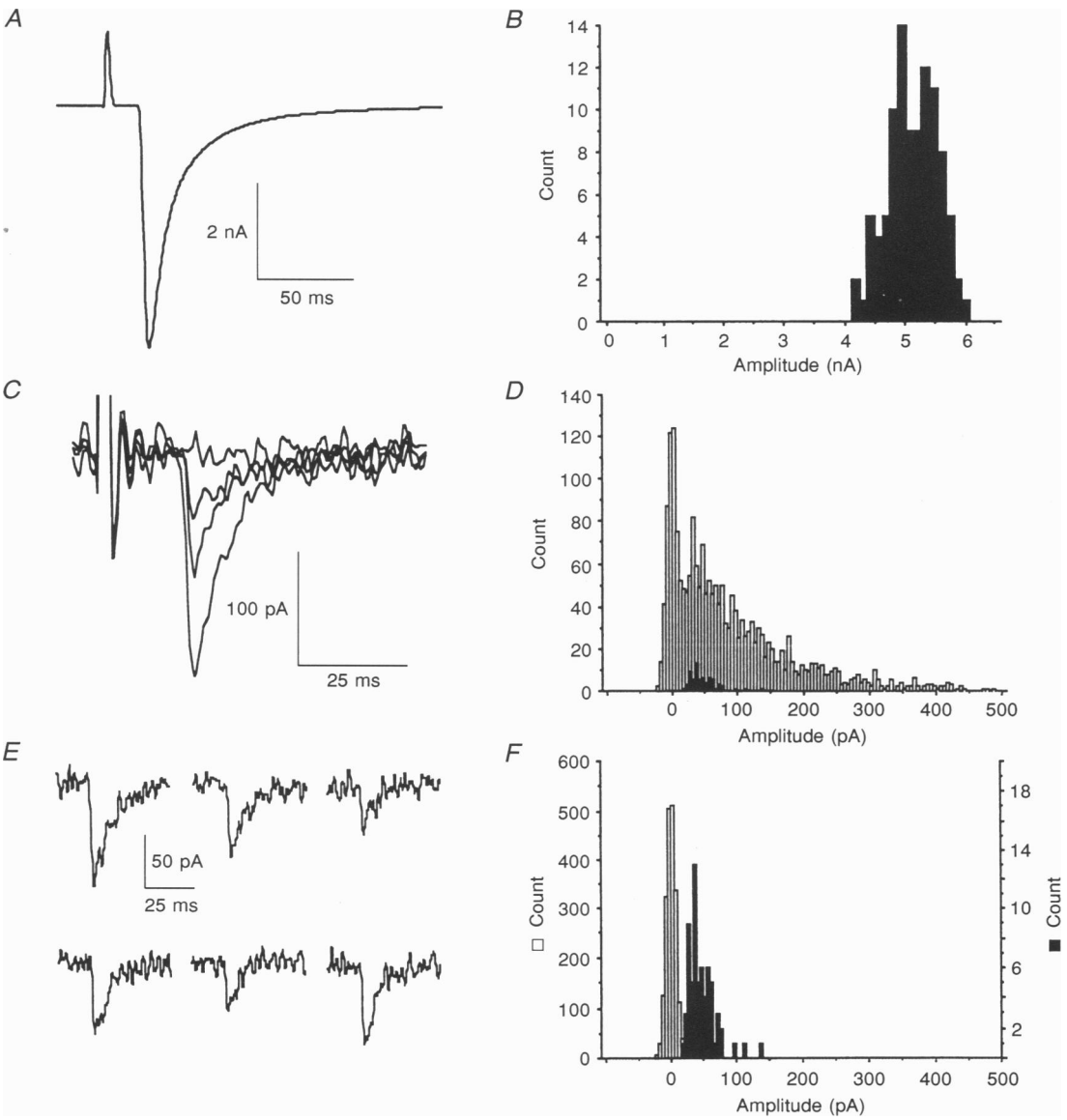

Figure 3. Evoked, cadmium-blocked and spontaneous EPSCs recorded from the same cell

A, evoked EPSC (average of 100 trials) recorded in normal Krebs solution (3·67 Hz stimulation; −80 mV membrane potential). *B*, histogram of peak amplitudes of the EPSC illustrated in *A* (mean = 5·1 nA; c.v. = 0·09; $n = 100$). *C*, evoked EPSCs recorded in the presence of 100 μM cadmium chloride, illustrating variability of EPSC amplitude and failure of response. *D*, histogram of cadmium-blocked EPSC peak amplitudes (open bars; mean = 85 pA; $n = 2000$). *E*, spontaneous EPSCs recorded in the presence of 100 μM cadmium chloride. *F*, amplitude histogram (filled bars, also shown in *D*; mean = 48 pA; $n = 66$) and corresponding noise (open bars; S.D. = 7 pA; $n = 2000$) for spontaneous EPSCs.

(approximately 25% of trials) were apparent (Fig. 3*C*). Histograms of the peak amplitudes of the evoked EPSCs under normal conditions and with added cadmium are illustrated in Fig. 3*B* and *D*, respectively. A clear separation between the 'failures' peak and the 'non-failures' response can be observed in the histogram illustrated in Fig. 3*D*. The corresponding background noise recorded in this cell is illustrated in Fig. 3*F*. In the same cell, a small number of spontaneous EPSCs ($n = 66$) were also recorded, and several examples are shown in Fig. 3*E*. A histogram of peak amplitudes of the spontaneous EPSCs is illustrated in Fig. 3*F* (and in Fig. 3*D*, filled bars). There is an obvious correspondence between the spontaneous EPSC histogram and the 'non-failures' peak in the histogram of evoked EPSCs (Fig. 3*D*). This observation provides supporting evidence that evoked release was reduced to the level of failures and one or several quanta.

Results for another cell are illustrated in Fig. 4, showing the time course of the decay phase of the evoked EPSC under normal conditions (Fig. 4*A* and *B*) and in the presence of 100 μM cadmium chloride (Fig. 4*C* and *D*). The decay phase of the evoked EPSC is described by the sum of two exponentials with time constants of 6·2 and 27·4 ms, respectively (Fig. 4*B*). Figure 4*D* shows that, in the presence of 100 μM cadmium chloride, the two component decay in the evoked EPSC persists, with time constants of 5·5 and 25·8 ms, respectively. This experiment was repeated in nine cells, and in all cases the two-phase decay persisted (Table 2). Neither the fast (τ_1) nor the slow (τ_2) time constants were significantly different under normal and low release conditions (paired t test, $P > 0{\cdot}05$).

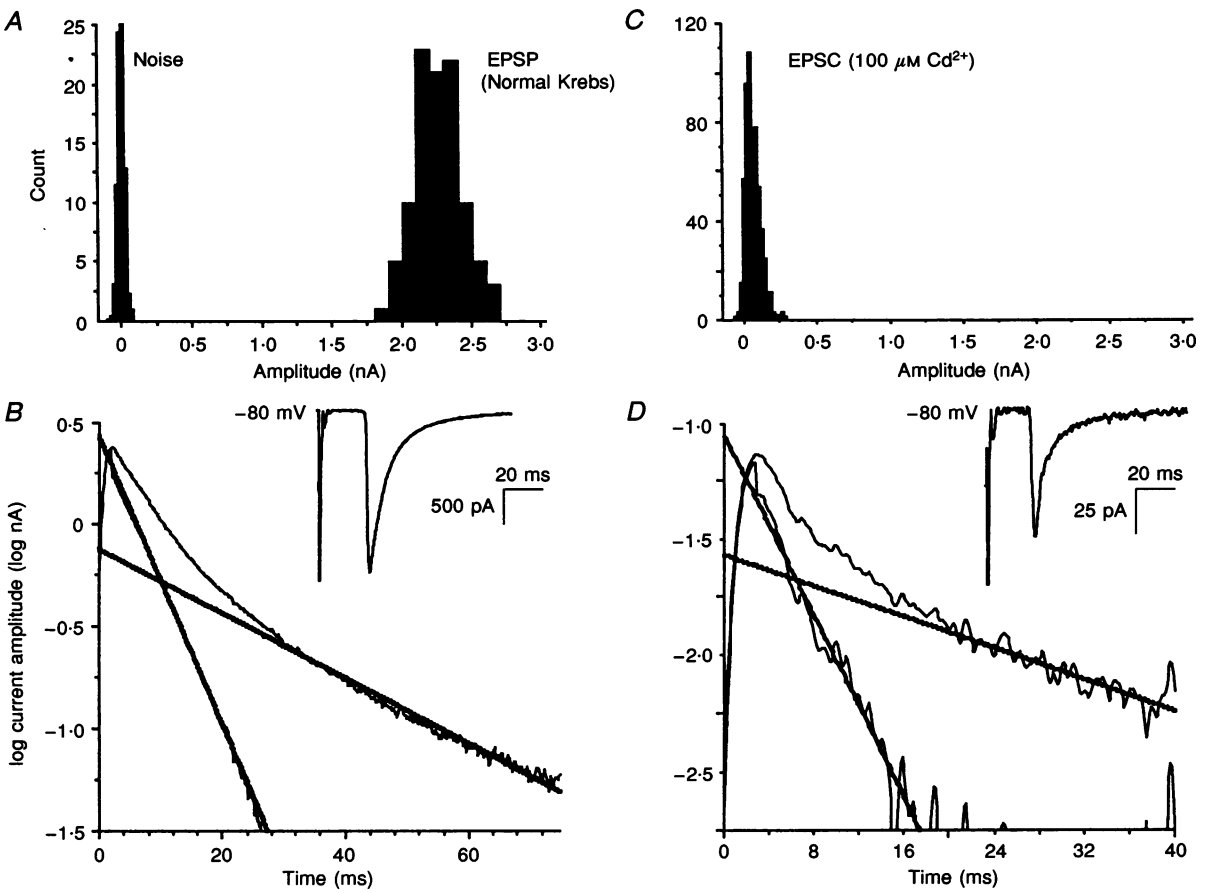

Figure 4. Comparison of the decay phase of evoked and cadmium-blocked EPSCs recorded in the same cell

A, histogram of the peak amplitudes for an evoked EPSC recorded in normal Krebs solution, and the corresponding noise (100 trials, 2·67 Hz stimulation, −80 mV membrane potential). *B*, semilogarithmic plot of the averaged evoked EPSC in normal Krebs solution. The decay phase of the synaptic current is well described by two time constants of 6·2 and 27·4 ms (straight lines). Inset shows the average of 100 EPSCs. *C*, amplitude histogram of the evoked EPSC peak amplitudes in the presence of 100 μM cadmium chloride. *D*, semilogarithmic plot of the cadmium-blocked evoked EPSC. The decay phase is well described by two exponential time constants of 5·5 and 25·8 ms. Inset shows the average of 700 EPSCs.

Table 2. Comparison of the time course of evoked EPSCs under normal and low release conditions

	EPSC peak amplitude (nA)		τ_1 (ms)		τ_2 (ms)	
Mean ± S.D.	3·84 ± 2·25	0·141 ± 0·057	6·9 ± 0·8	6·4 ± 0·9	30·6 ± 4·3	33·0 ± 10·8
Range	1·16–8·90	0·052–0·223	6·2–8·7	4·6–8·2	23·2–35·4	20·4–53·1

Data are from 9 cells held at membrane potentials between −50 and −80 mV. Parameters are given for EPSCs recorded in normal Krebs solution and after the addition of 100 μM $CdCl_2$.

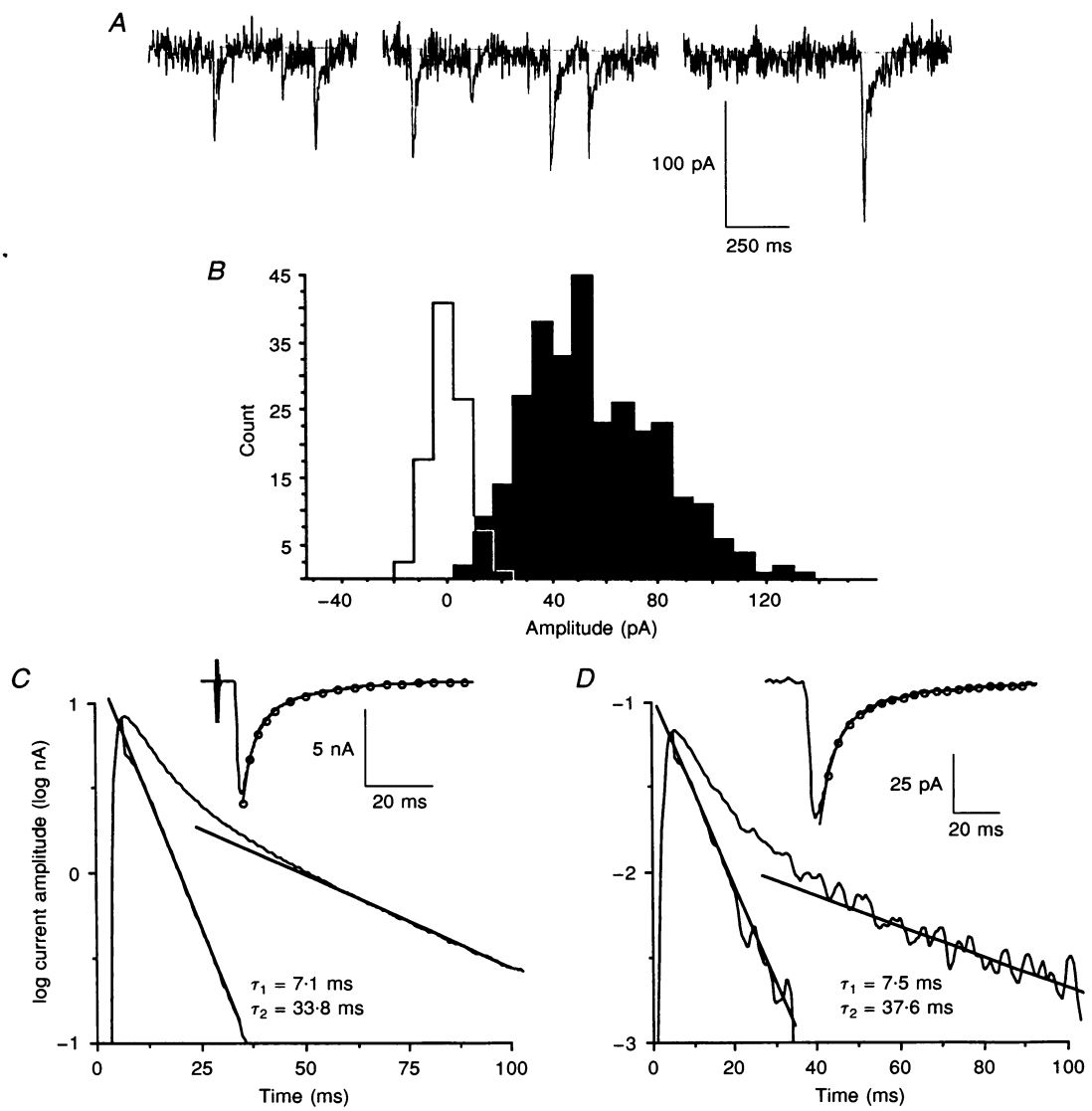

Figure 5. Evoked and spontaneous EPSCs recorded in the same cell

A, selected traces showing spontaneous EPSCs recorded in normal Krebs solution (−80 mV membrane potential). *B*, amplitude histograms of spontaneous EPSCs (filled bars; mean = 57 pA; c.v. = 0·42; n = 299) and corresponding noise (open bars). *C*, semilogarithmic plot of the decay phase of the evoked EPSC (inset; average of 100 trials). *D*, semilogarithmic plot of the decay phase of spontaneous EPSC (inset; average of 241 trials). The EPSC decay phases in both *C* and *D* were well fitted by the sum of two exponentials (○ in insets). Straight lines superimposed on semilogarithmic plots in *C* and *D* indicate the fast and slow exponential components of the decay phase.

Properties of spontaneous quantal EPSCs

As previously observed (Rang, 1981), spontaneous miniature EPSCs occur infrequently in submandibular ganglion cells. Our attempts to increase the frequency of spontaneous EPSCs using standard procedures, such as hypertonic solutions (Bekkers, Richerson & Stevens, 1990) or high potassium solutions (Van der Kloot, 1991), proved unsatisfactory. Hypertonic solutions (up to 450 mmol kg^{-1}) failed to significantly increase the frequency of spontaneous events. High potassium levels significantly increased the noise, and reduced the stability of the recordings. However, in four experiments using normal Krebs solution, we were able to record both the nerve-evoked EPSC and adequate numbers of spontaneous EPSCs under low-noise conditions, and compare their properties.

The results for one cell are illustrated in Fig. 5. Figure 5*A* illustrates several spontaneous EPSCs recorded in this cell. It is apparent that there are large differences between the peak amplitudes of spontaneous EPSCs. This variability is illustrated in the histogram of EPSC peak amplitudes constructed from 299 spontaneous EPSCs recorded in this cell (Fig. 5*B*). Also plotted in Fig. 5*B* is a histogram of the backgound noise. The variability in peak amplitude of the spontaneous EPSCs greatly exceeds the contaminating noise. Following subtraction of the noise variance, the c.v. of the spontaneous EPSC peak amplitudes was calculated to be 0·42.

Figures 5*C* and *D* compare the time course of the evoked and spontaneous EPSCs recorded in this cell. The time course of the evoked EPSC was well fitted by a double-exponential decay, with $\tau_1 = 7{\cdot}1$ ms and $\tau_2 = 33{\cdot}8$ ms. These time constants were well matched by those fitted to the decay phase of the averaged ($n = 299$) spontaneous EPSC, with $\tau_1 = 7{\cdot}5$ ms and $\tau_2 = 37{\cdot}6$ ms (Fig. 5*D*).

Spontaneous EPSCs were recorded in a total of five cells, at a membrane potential of −80 mV. The mean peak amplitude of spontaneous EPSCs for all five cells was 81 pA, and the mean c.v. was 0·37. In four of these cells, evoked EPSCs were also recorded for time course comparison with the spontaneous EPSCs. In all four cells, the time course of the averaged spontaneous EPSCs exhibited a double-exponential decay phase, similar to the two-phase decay of the evoked EPSCs. The mean time constants for the spontaneous EPSCs were $\tau_1 = 8{\cdot}3 \pm 1{\cdot}2$ and $\tau_2 = 38{\cdot}0 \pm 9{\cdot}6$, and the mean time constants for the evoked EPSCs were $\tau_1 = 7{\cdot}1 \pm 0{\cdot}5$ and $\tau_2 = 34{\cdot}7 \pm 0{\cdot}7$ ($n = 4$). Neither the fast (τ_1) nor the slow (τ_2) time constants were significantly different for the evoked and spontaneous EPSCs (paired t test, $P > 0{\cdot}05$).

DISCUSSION

In the present experiments we have studied quantal transmission, and investigated the hypothesis that evoked and spontaneous quantal EPSCs are generated by different populations of postsynaptic channels in submandibular ganglion cells.

Evoked EPSCs were studied at the level of one or several quanta by reducing release to a substantial level of failures. Under these conditions, a double-exponential decay of the EPSC was present. This extends, to the quantal level, the result obtained by Rang (1981) in which the peak amplitude of the evoked EPSC was reduced to approximately 10% of control value by decreasing the calcium : magnesium ratio in the perfusate. However, in contrast to Rang (1981), our results demonstrate that the double-exponential decay is also present in the spontaneously occurring EPSCs. Furthermore, there is good agreement between the two time constants fitted to the decay time course of the spontaneous EPSCs and the evoked EPSCs recorded in the same cell. The most likely explanation for the inconsistency between our result and that of the previous study is that the slower time constant component can be clearly resolved only under conditions of low noise, following the averaging of large numbers of spontaneous EPSCs. This condition was achieved in our study for very few cells, since the rate of spontaneously occurring EPSCs is extremely low in the submandibular ganglion.

Thus, we conclude that the spontaneous and evoked EPSCs are generated by activation of the same postsynaptic channels, and that there is no evidence for a distinction between nerve-evoked and spontaneously occurring quantal EPSCs. Although it was previously considered likely that there are two separate populations of acetylcholine-gated channels in submandibular ganglion cells, our results re-open the possibility of only a single population of receptor channels with complex kinetics (Colquhoun & Sakmann, 1985; Mathie *et al.* 1987; Derkach, North, Selyanko & Skok, 1987; Sargent, 1993). This possibility was also considered by Yawo (1989), following the demonstration that the fast and slow kinetic components of both the EPSC and the acetylcholine-gated channels exhibit identical voltage sensitivities in mouse submandibular ganglion cells.

The mean peak amplitude of spontaneous EPSCs recorded in the present study was 81 pA at a membrane potential of −80 mV. The single-channel conductance for acetylcholine-gated channels in submandibular ganglion cells is approximately 30 pS at negative membrane potentials (Rang, 1981; Yawo, 1989). Thus, the mean spontaneous EPSC represents the opening of approximately thirty-five acetylcholine channels. At a membrane potential of −80 mV, the peak amplitude of evoked EPSCs varied enormously between cells, ranging from 1·2 to 9·8 nA (mean = $4{\cdot}6 \pm 2{\cdot}6$ nA, $n = 23$ cells). In five cells, both spontaneous and evoked EPSCs were recorded. Assuming that the evoked EPSC is composed of the sum of quantal EPSCs with mean amplitude equal to that of the spontaneous EPSCs, the mean quantal content of the

evoked EPSCs in these five cells ranged from 16 to 136 (mean = 76 ± 49). It is likely that this large range is primarily due to differences in the total number of synaptic contacts formed between single preganglionic fibres and submandibular ganglion cells (Lichtman, 1977; Rang, 1981; Callister *et al.* 1995).

The present study is the first to demonstrate that there is considerable variability in the peak amplitude of spontaneous quantal EPSCs recorded in submandibular ganglion cells. The mean c.v. of EPSC peak amplitudes is large (mean = 0·37, $n = 5$ cells), despite a lack of spread due to electrotonic attenuation of EPSCs in these cells. It remains to be determined how much of this large variability is due to differences in mean EPSC amplitude between release sites (perhaps due to differences in the numbers of receptors), and how much is due to intrinsic variability at each release site (Edwards, Redman & Walmsley, 1976; Hirst & McLachlan, 1984; Walmsley, Edwards & Tracey, 1988; Bekkers *et al.* 1990; Faber, Young, Legendre & Korn, 1992; Walmsley, 1991, 1993; Sargent, 1993; Bekkers, 1994).

Ascher, P., Large, W. A. & Rang, H. P. (1979). Studies on the mechanism of action of acetylcholine antagonists on rat parasympathetic ganglion cells. *Journal of Physiology* **295**, 139–170.

Bekkers, J. M. (1994). Quantal analysis of synaptic transmission in the central nervous system. *Current Opinion in Neurobiology* **4**, 360–365.

Bekkers, J. M., Richerson, G. B. & Stevens, C. F. (1990). Origin of variability in quantal size in cultured hippocampal neurons and hippocampal slices. *Proceedings of the National Academy of Sciences of the USA* **87**, 5359–5362.

Callister, R. J., Keast, J. R. & Walmsley, B. (1995). The physiological and structural basis of synaptic transmission in rat submandibular ganglion cells. *Proceedings of the Australian Neuroscience Society* **6**, 92.

Callister, R. J. & Walmsley, B. (1994*a*). The time course of quantal synaptic currents in rat submandibular ganglion cells. *Society for Neuroscience Abstracts* **20**, 620.14.

Callister, R. J. & Walmsley, B. (1994*b*). Two-electrode voltage clamp recordings of quantal synaptic currents in rat submandibular ganglion cells. *Proceedings of the Australian Neuroscience Society* **5**, 78.

Colquhoun, D. & Sakmann, B. (1985). Fast events in single-channel currents activated by acetylcholine and its analogues at the frog muscle end-plate. *Journal of Physiology* **369**, 501–557.

Derkach, V. A., North, R. A., Selyanko, A. A. & Skok, V. I. (1987). Single channels activated by acetylcholine in rat superior cervical ganglion. *Journal of Physiology* **388**, 141–151.

Derkach, V. A., Selyanko, A. A. & Skok, V. I. (1983). Acetylcholine-induced current fluctuations and fast excitatory post-synaptic currents in rabbit sympathetic neurones. *Journal of Physiology* **336**, 511–526.

Edwards, F. R., Redman, S. J. & Walmsley, B. (1976). Non-quantal fluctuations and transmission failures in charge transfer at Ia synapses on spinal motoneurones. *Journal of Physiology* **259**, 689–704.

Faber, D. S., Young, W. S., Legendre, P. & Korn, H. (1992). Intrinsic quantal variability due to stochastic properties of receptor-transmitter interactions. *Science* **258**, 1494–1498.

Hirst, G. D. S. & McLachlan, E. M. (1984). Post-natal development of ganglia in the lower lumbar sympathetic chain of the rat. *Journal of Physiology* **349**, 119–134.

Kawa, K. & Roper, S. (1984). On the two subdivisions and intrinsic synaptic connections in the submandibular gland of the rat. *Journal of Physiology* **346**, 301–320.

Kuba, K. & Nishi, S. (1979). Characteristics of fast excitatory postsynaptic current in bullfrog sympathetic ganglion cells. *Pflügers Archiv* **378**, 205–212.

Lichtman, J. W. (1977). The reorganization of synaptic connexions in the rat submandibular ganglion during post-natal development. *Journal of Physiology* **273**, 155–177.

Mathie, A., Cull-Candy, S. G. & Colquhoun, D. (1987). Single channel and whole-cell currents evoked by acetylcholine in dissociated sympathetic neurons of the rat. *Proceedings of the Royal Society* B **232**, 239–248.

Rang, H. P. (1981). The characteristics of synaptic currents and responses to acetycholine of rat submandibular ganglion cells. *Journal of Physiology* **311**, 23–55.

Sargent, P. B. (1993). The diversity of neuronal nicotinic acetylcholine receptors. *Annual Review of Neuroscience* **16**, 403–443.

Van der Kloot, W. (1991). The regulation of quantal size. *Progress in Neurobiology* **36**, 93–130.

Walmsley, B. (1991). Central synaptic transmission: Studies at the connection between primary afferent fibres and dorsal spinocerebellar tract neurones in Clarke's column of the spinal cord. *Progress in Neurobiology* **36**, 391–423.

Walmsley, B. (1993). Quantal analysis of synaptic transmission. In *Electrophysiology: A Practical Approach*, ed. Wallis, D. I., pp. 109–141. Oxford University Press, Oxford.

Walmsley, B., Edwards, F. R. & Tracey, D. J. (1988). Nonuniform release probabilities underlie quantal synaptic transmission at a mammalian excitatory central synapse. *Journal of Neurophysiology* **60**, 889–908.

Yawo, H. (1989). Rectification of synaptic and acetylcholine currents in submandibular ganglion cells. *Journal of Physiology* **417**, 307–322.

Acknowledgements

We would like to thank Drs James Brock and Jeff Isaacson for helpful comments on the manuscript. This work was supported by grants from the National Health and Medical Research Council of Australia and the Clive and Vera Ramaciotti Foundations. Dr R. J. Callister is currently an NH&MRC Australian Postdoctoral Fellow.

Received 10 March 1995; accepted 5 July 1995.